Australian Journal of Chemistry 73 (8): 669-676 (2020)

Graphical Abstract

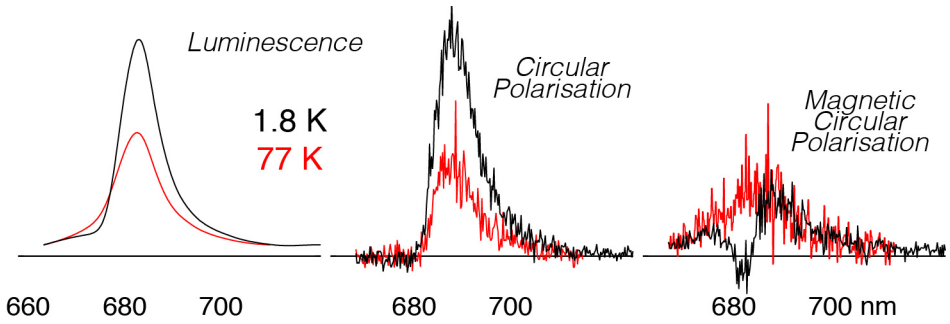

Table of contents (TOC) abstract

Studies of *isolated* reaction center preparations of PS II have been pivotal in the development of models of both the coupling between its pigments and the process of charge separation. A number of key puzzles remain in our understanding of these important systems. We apply new and powerful optical techniques (CPL and MCPL) and by means of an exciton analysis, point to key new ideas.

Australian Journal of Chemistry 73 (8): 669-676 (2020)

New Perspectives on Photosystem II Reaction Centres

Jeremy Hall[A], *Rafael Picorel*[B], *Nicholas Cox*[A], *Robin Purchase*[A] *and Elmars Krausz*[A]

[A] Research School of Chemistry, Australian National University, Canberra, Australia

[B] Estacion Experimental de Aula Dei (CSIC), Avda. Montañana 1005, 50059-Zaragoza, Spain

Email: elmars.krausz@anu.edu.au Fax:+61-2-6125-0750

Running Head: New Perspectives PS II RCs

Keywords: Absorption, Circular Dichroism, Luminescence, Photosystem II, Reaction Centre.

Abbreviations:

Photosystem II - PSII

Ultraviolet/Visible - UV/Vis

Circular Dichroism - CD

Magnetic Circular Dichroism - MCD

chlorophyll-a - *Chl-a*

Pheophytin-a - *Pheo-a*

Supplementary Information - SI

ABSTRACT

We apply the differential optical spectroscopy techniques of Circular Polarisation of Luminescence (CPL) and Magnetic CPL (MCPL) to the study of isolated reaction centres (RCs) of Photosystem II (PS II). The data and subsequent analysis provide insights into aspects of RC chromophore site energies, exciton couplings, and heterogeneities. CPL measurements are able to identify weak luminescence associated with the unbound chlorophyll-a (*Chl-a*) present in the sample. The overall sign and magnitude of the CPL observed relates well to the Circular Dichroism (CD) of the sample. Both CD and CPL are reasonably consistent with modelling of the RC exciton structure. The Magnetic CPL (MCPL) observed for the free *Chl-a* luminescence component in the RC samples is also easily understandable, but the MCPL seen near 680 nm at 1.8 K is anomalous, appearing to have a narrow, strongly *negative* component. A negative sign is inconsistent with MCPL of (exciton coupled) Q_y states of either *Chl-a* or *Pheo-a*. We propose that this anomaly may arise as a result of luminescence from a transient excited state species created following photo-induced charge separation within the RC. A comparison of CD spectra and modelling of RC preparations having a different number of pigments suggests that the non-conservative nature of CD spectra observed is associated with the 'special pair' pigments P_{D1} and P_{D2}.

Introduction

There have been a number of interesting recent developments in the spectroscopy of Photosystem II (PS II) relevant to the fundamental charge separation processes. These include the identification of vibrational coherence [1] following femtosecond pulse excitation of isolated reaction centres (RCs). There has also been the unexpected involvement of far-red absorbing chlorophylls (*chlorophyll-f* and *chlorophyll-d*) in charge separation processes in some cyanobacteria [2]. The reduction of the lowest energy (Q_y) excitation in these chlorophylls significantly reduces the driving potential available in subsequent chemical transformations.

The reaction centre of PS II is unique in its ability to photo-generate the (biologically extreme) oxidative potential needed to drive water-splitting in nature. An extensive range of spectroscopic measurements have been made on PS II over the last three decades [3]. These have been performed on purified protein assemblies sourced from a range of photosynthetic organisms. Although the basic content and layout of the photoactive pigments and redox components contained within PS II is well understood through crystallographic and other studies, there remains a notable lack of consensus regarding some of the fundamental processes, spectroscopic assignments and functions in this critical enzyme. To help resolve some of these issues, we introduce and discuss preliminary results generated by two novel low-temperature optical measurements. These techniques have not previously been applied to the study of RCs. We utilise a relatively simple theoretical model to account for exciton coupling between the photoactive chromophores in RCs, including the significant effects of heterogeneity of their pigment site energies. We interpret these results and relate them to some of the measurements that have been made on RCs made using other spectroscopic techniques.

The minimal PS II assembly capable of oxygen evolution is a PS II core complex, as shown in Fig.1(b). The core complex incorporates D1, D2 and $Cytb_{559}$ protein helices of the RC as well as those of the CP43 and CP47 proximal light harvesting antennae. It also contains a range of other protein components. PS II water splitting capacity is incorporated in the manganese-stabilising protein PsbO which hosts the self-assembled $CaMn_4O_5$ catalytic centre. A PS II core complex is a large and fragile assembly and many studies have resorted to measurements of the isolated PS II RC [4], a simpler preparation containing only the D1, D2 and $Cytb_{559}$ proteins as shown in Fig. 1(a). An isolated RC retains no catalytic function but performs repetitive charge separation followed by recombination following absorption of a photon. It does *not* undergo the complex multi-photon redox transformations of a functional PS II core. Although isolated RC preparations have been shown to be variable and heterogeneous [5], the absence of the many metastable photo-chemical steps which plague any study of PS II core complexes means that they have been utilised in many studies. A very wide range of spectroscopies have been performed on isolated RCs. A multi-spectral analysis [6] of a

range of optical spectroscopic measurements on RCs led to the first widely accepted description of the excitonic structure of the reaction centre of PS II. The excitonic assignments proposed have been paralleled and refined by other workers [7] although they have been criticised by one group [8].

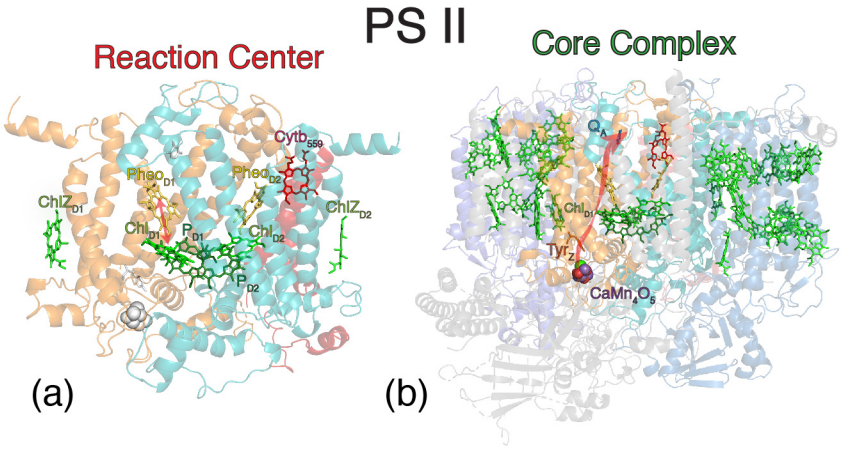

Fig. 1

The structure on the right (b) is a schematic of the crystal structure of the PS II core complex of eukaryotic Cyanidium caldarium [9], visualised using PyMol open-source software by Julien Langley. The expanded view (a) of the RC on the left utilises a slightly rotated perspective that enables better visualisation of the key RC pigments. The relevant protein helices are D1 (orange), D2 (cyan) and $Cytb_{559}$ (red). Chl-a pigments are shown in green with the special pair pigments P_{D1} and P_{D2} being darker green. Pheo-a molecules are yellow and the $Cytb_{559}$ heme is red. For the PS II core complex (b), the CP43 peripheral light harvesting assembly (left) is mauve whilst the CP47 assembly (right) is blue. Other auxiliary proteins in the core complex are shown in grey. The red arrow displayed in the PS II core complex traces the multi-step electron transfer path from the catalytic $CaMn_4O_5$ site to the plastoquinone Q_A via the secondary donor Tyr_Z, the primary donor Chl_{D1} and the primary acceptor $Pheo_{D1}$. In the RC, Tyr_Z, the $CaMn_4O_5$ and Q_A are shaded light grey, indicating that they are missing or inactive compared to the same redox component in a core complex. The charge separation and rapid recombination process between Chl_{D1} and $Pheo_{D1}$ in an RC is indicated by the shorter, red, double-headed arrow.

Circular Polarisation of Luminescence (CPL) measurements, particularly those performed at low temperatures [10], serve as a natural partner to Circular Dichroism (CD) studies. As fluorescence in the condensed phase most often ensues from the lowest excited state(s) of a molecule (or coupled chromophore assembly) CPL probes the detailed nature of these (photochemically and photophysically) important lowest energy excited states [11]. The low-temperature CPL technique was first developed to study the peripheral light-harvesting antennae of PS II i.e. CP43 [10a] and CP47 [10b]. These measurements helped to clarify excitation transfer processes and, with the assistance of

modelling, provided definitive assignments of site energies and heterogeneity within these relatively complex arrays of ~12-15 *Chl-a* chromophores.

Magnetic CPL (MCPL) is the luminescence analogue to Magnetic CD (MCD). For either CD or MCD the fractional circular polarisation ρ_A is defined as the ratio of the difference of left and right circularly polarised light, A_L and A_R, divided by absorption. This anisotropy ratio has been labelled $\Delta A/A$. The absorbance A is usually defined as the average of absorption in left and right circularly polarised light. In most cases, $|\rho| << 1$ and thus $A_L \sim A_R$ and $(A_L+A_R)/2$ corresponds to the absorption spectrum. With the definition in (1) the extremal values of ρ are +2 and -2.

$$\rho_A = \Delta A/A = (A_L-A_R)/[(A_L+A_R)/2] \quad (1)$$

An equivalent definition for the ratio of CPL and MCPL to luminescence spectra ρ_E is

$$\rho_E = \Delta I/I = (I_L-I_R)/[(I_L+I_R)/2] \quad (2)$$

For a single, purely electronic transition, ρ_A is identical to ρ_E [12]. Any mismatch indicates that either (a) the luminescence spectrum may not be fully representative of the ensemble of absorbing species (perhaps owing to heterogeneity) (b) that multiple electronic transitions are involved (c) that the transition is vibronic (i.e. is outside the crude adiabatic Born-Oppenheimer approximation see reference [12] Chapter 3) or (d) that the initially formed excited state changes to a different structure (owing to photophysical or photochemical changes) within the lifetime of the excited state.

MCPL spectra of photosynthetic assemblies have remained unreported until now, although MCD spectra of a number of photosynthetic systems have been reported [13]. ρ_E for isolated *Chl-a* or *Pheo-a* can be expected to mirror ρ_A, with absorption and luminescence known to involve the lowest energy, Q_y state. Exciton coupling and other factors [14] lead to changes in the magnitude of ρ_A for the Q_y state in MCD measurements. The amplitude of Q_y MCD is linear in the applied magnetic field and is also temperature independent, identifying it as an MCD B-term [12]. A remarkably strong reduction of ρ_A for the Q_y state MCD of RC-6 near 680 nm was reported some time ago [15]. There is a notable similarity to the P680 laser-induced transient changes characteristic of RC-6 charge separation and the so-called 'MCD deficit'. However, a fundamental understanding of the variations of the corresponding MCD B-term is incomplete [14] and remains a subject of on-going interest and research.

Method

Specialised Spectrometer System

The single optical spectrometer system utilised was capable of making high-precision measurements of absorption, fluorescence, excitation, CD, MCD, CPL as well as MCPL spectra has been previously described [16]. This system has the advantage that simultaneous and/or parallel spectroscopic measurements can be made on a single biochemical sample. Photosynthetic protein preparations can be both variable and fragile. Being able to measure the same sample in the same spectrometer system, without having to thermally cycle or otherwise change the sample is a significant advantage. Protocols, procedures and sample handling systems have been developed that prevent the sample from being degraded by exposure to non-actinic light [16b, 16c, 17]. Samples can, if necessary, be loaded whilst only being exposed to light of wavelength longer than 750 nm. The period for which the sample is at ambient temperatures or exposed to air is also minimised.

In any optical spectrometer developed to measure very small levels of dichroism, in either absorption or luminescence, there is often a problem with variable baselines, offsets and other artefacts. When the sample utilised is a low-temperature frozen glass, these problems can become severe. Typically, artefactual dichroism is induced by unintended birefringence of the components in the optical pathway. This birefringence can be induced by even small levels of strain in the optical components of the system (lenses/windows/polarisers) or in the sample itself. For CD (or equivalently MCD) measurements, the presence of residual signals can be identified by (non-zero values of) dichroism measurements in regions of no absorption. For the corresponding CPL measurements, there is no such recourse, as residual circular polarisation of (no) luminescence cannot be monitored. For MCPL, a very useful procedure is to reverse the applied magnetic field, which reverses the sign of the MCPL signal but not that of any CPL (or artefactual signals).

For CPL measurements to be of value, it is critical to develop and apply procedures that can quantify the presence of artefacts, so as to eliminate or at least minimise them. Such procedures were pioneered in the CPL papers on CP43 and CP47 [10]. In the current work, the linearity of the MCD/MCPL signal with applied magnetic field as well as the reversal of its sign with applied field was verified, to the extent that the signal-to-noise available in spectra allowed.

A detailed description of the properties and biochemical preparation of RC-6 and RC-6 samples sourced from spinach has been described in detail[18]. The samples used for optical experiments were prepared in a similar way to those for the ΔFLN experiments above, except that that they were diluted to ~ 55% with a 1:1 glycerol:ethylene glycol mixture (v/v) as glassing agent. Specialised strain-free, cylindrical fused-quartz sample cells of 12 mm diameter and 0.2 mm to 1 mm in pathlength were used. These cells have also been described [16c, 17].

Results and Discussion

CPL and MCPL Spectra

In an analysis of CPL and MCPL it is most helpful to be able to compare luminescence, CPL, MCPL spectra with corresponding absorption, CD and MCD spectra. A detailed comparison of CD and CPL spectra was critical in the analysis of spectra of CP43 [10a] and CP47 [10b]. We report CPL and MCPL data only for RC-6, as it appears to be more photo-stable than RC-5 and less heterogeneous. Clear evidence of RC-5 heterogeneity is provided by a characteristic ~10% reduction of its $Cytb_{559}$ chromophore, whereas in RC-6 $Cytb_{559}$ is fully oxidised [19]. Additionally, RC-6 has been the RC system studied most in reports of coherence in transient pump-probe experiments [1a].

Fig 2. compares absorption, fluorescence, CD and MCD spectra of RC-6 with CPL and MCPL measurements. All spectra were made on the same sample or sample preparation. They were all taken on the same spectrometer system and in the same superconducting magnet cryostat. Luminescence, CPL and MCPL spectra were taken simultaneously, as were absorption, CD and MCD spectra. CD and MCD spectra were taken before and after the strong laser illumination necessary to record CPL and MCPL spectra to quantify any changes in the sample. These were found to be minimal.

Spectra were also taken with a *reversed* magnetic field, which must reverse the sign of a genuine MCPL signal (as it does for the MCD signal) but leaves the CPL (and equivalently the CD) and corresponding luminescence (or absorption) unchanged. Subtraction of these 'normal' and 'reversed field' spectra provides the MCPL spectrum whilst addition of the two spectra provides the CPL spectrum. CPL spectra recorded at zero applied field were seen to be identical to those determined by the addition of normal and reverse field spectra. The amplitude of the luminescence spectrum decayed slightly upon extended laser illumination at 1.8 K without a significant change of shape in the spectrum. This intensity change effect was corrected for when averaging over many spectra. Averaging was necessary to improve signal-to-noise to a useful level.

The CPL and MCPL spectra in Fig. 2 were averaged over ~ 4-10 scans. As mentioned above, CPL and MCPL spectral components are additive. To exclude artefacts associated with any gradual degradation of the sample, spectra were recorded with the negative field spectrum

taken first and compared with pairs where the positive magnetic field spectra were taken first. This precaution was taken as MCPL spectra of RC-6 appeared to be distinctly anomalous in the 680 nm region (Fig. 2).

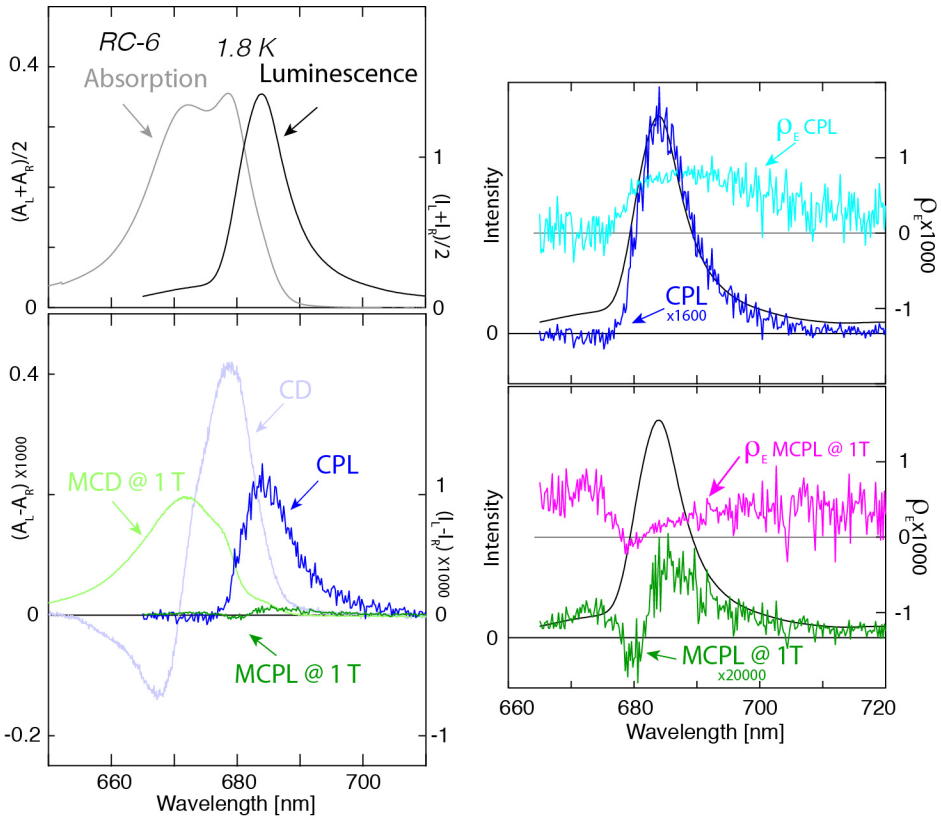

Fig. 2

The upper part of the l.h. panel shows overlays of RC-6 absorption and luminescence spectra (grey and black, respectively) taken at 1.8 K. Corresponding CD and MCD spectra (light blue and light green) are compared with CPL and MCPL (blue and green) spectra in the lower section. MCD and MCPL spectra are normalised to an applied magnetic field of 1 T. The r.h. panels show CPL (blue) and MCPL (green) (I_L-I_R) spectra overlaid with the luminescence spectrum scaled arbitrarily as (I_L+I_R)/2. To match the peak height of the luminescence spectrum at 685 nm, the CPL spectrum (I_L-I_R) has been multiplied by 1600. Similarly, the MCPL at 1 T has been multiplied by 20000, to match the luminescence intensity in the 670 nm region. The r.h. scale displays ρ_E, the ratio of CPL to luminescence intensities (pale blue) and MCPL at 1 T to luminescence intensities (pale green) as defined in Eqn. (2). Luminescence spectra were taken by illuminating with a Verdi G laser at 532 nm and an excitation fluence of ~100 mW/cm^2.

The absorption, CD and MCD spectra shown in Fig. 2 are in good agreement with those previously reported [7a, 19-20]. The main features of the absorption and CD spectra have been accounted for by modelling [6-7] the exciton coupling interactions between the pigments in the

RC. Utilising the exciton mechanism, and allowing coupling only between Q_y excitations, leads the Q_y CD to be constrained to show overall equal positive and negative components, i.e. summing to zero net area. The CD generated by this mechanism is called conservative. However, both RC-6 and RC-5 display a similar and significant net positive CD component. This non-conservative behaviour has been previously noted but cannot be easily accounted for by the (much smaller) CD of isolated *Chl-a* or to coupling to other porphyrin excitations.

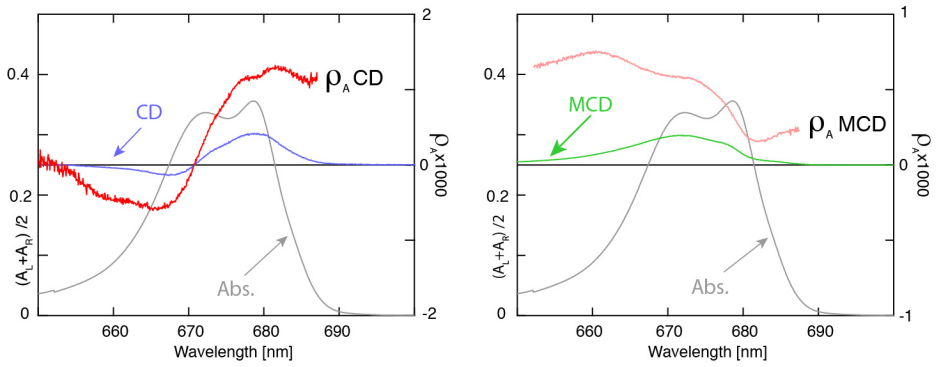

Fig. 3

Left: Absorption of RC-6 (grey) compared to CD (blue). Also shown is the anisotropy ratio ρ_A (red) of the CD to absorbance. Right: The same absorption spectrum compared to the MCD spectrum for an applied field of 1 T (green), and the MCD ρ_A (orange) for an applied field of 1 T. The ρ_A curves are on the same (dimensionless) scale as the CD and MCD spectra. These ratios are analogous to the CPL and MCPL ρ_E anisotropy ratios of Fig.2. Absorption/CD/MCD spectra were recorded simultaneously at 1.8 K.

The ρ_A of RC-6 in MCD varies significantly across the Q_y absorption region (Fig. 3). The spectral region dominated by the ChlZ pigments (~660 – 675 nm) has a value of ρ_A in a 1 T field of ~0.4-0.6 x 10^{-3} (Fig. 3). This is close to the value seen for *Chl-a* in ether at room temperature of ρ_A=0.38 x 10^{-3} [21]. In contrast and as previously noted [15], the MCD spectrum of isolated RCs shows a very strongly reduced MCD amplitude in the 680 nm region. We have previously noted that the reduction of this MCD to absorption ratio, also called the 'MCD deficit', was phenomenologically related to the role the *Chl-a* performed in a photosynthetic assembly [2a, 22]. Pigments involved in charge separation have a significantly reduced MCD. A theoretical understanding of this 'MCD deficit' is still lacking [14b].

We emphasise again that for any given purely electronic transition, the CD (or MCD) ρ_A and ρ_E values are identical. They are constrained to be so [12] as they involve the same transition dipole matrix elements. Luminescence at low temperatures in the condensed phase normally

arises only from the lowest excited state of a chromophore or excitonically coupled assembly of chromophores. Therefore, the ρ_E value in CPL (or MCPL) is expected to be constant across a spectral profile, if luminescence arises from a single electronic sate. Fig. 2 shows, very clearly, that ρ_E is not constant in RC-6 for either the CPL or MCPL spectra.

The sign of the main RC-6 CPL feature is positive, as expected. It has the same sign as the lowest energy CD feature. The CPL ρ_E is ~0.7 x 10^{-3} and reasonably constant across the main luminescence profile. Its magnitude is also in reasonable agreement with the CD to absorption ratio ρ_A~1 x 10^{-3} in the low energy region of absorption (Fig. 3). The remaining discrepancy seen here is likely to be, at least partly, due to the non-correlated heterogeneity of pigment site energies. The quantum efficiency of fluorescence in RC-6 is around 10% and those sites that emit may not be equivalently represented in absorption.

The region at shorter wavelengths (660 nm to 675 nm) exhibits no CPL to within the signal-to-noise available. Luminescence in this region can be attributed to a small amount of 'free' *Chl-a* present in the sample, these pigment(s) are not excitonically coupled to other pigments. Absorption of this (monomeric) Q_y component will then inherently exhibit only very weak (monomeric) CD and thus have correspondingly weak CPL.

The CPL ρ_E in the region beyond 700 nm gradually vanishes. This region corresponds to the (non-resonantly excited) vibrational sideband luminescence region of RC-6. We have shown that corresponding Q_y vibrational sideband CPL in CP43 is weak, owing to the process of vibronic localisation [10a]. Thus, we attribute the reduction seen in CPL for the long wavelength region in Fig. 2 to the same vibronic localisation effect.

In comparison to the CPL spectrum, the MCPL spectrum of RC-6 exhibits a radically different profile to that of the luminescence spectrum. The MCPL spectrum in Fig. 2 has been scaled to match the luminescence intensity in the 670 nm region, this requires a factor of 2 x 10^4. This factor determines the MCPL ρ_E at 1T applied field near 670 nm to be ~0.5 x 10^{-3}. The value of ρ_E appears to be ~ 0.3 x 10^{-3} in the spectral range from 690 nm to 720 nm, but the data is relatively noisy. In the spectral range from 675 nm to 685 nm the value of ρ_E drops markedly and even becomes *negative* at 680 nm.

The 680 nm luminescence feature has ρ_E = -0.3 x 10^{-3}. It has only half the width of the main luminescence feature and contributes ~10% of the total luminescence (see SI for details). It's CPL appears to be negligible. There are no known examples where the MCD (and equivalently MCPL) of a Q_y chlorin excitation is negative and there is no clear mechanism whereby a chlorin Q_y excitation could exhibit a negative MCD or MCPL. The Q_y ρ_A in 1 T MCD of RC-6 drops to 0.15 x 10^{-3} at 682 nm and thus exhibits the strongest 'MCD deficit' to be identified, but ρ_A always remains positive (Fig. 3).

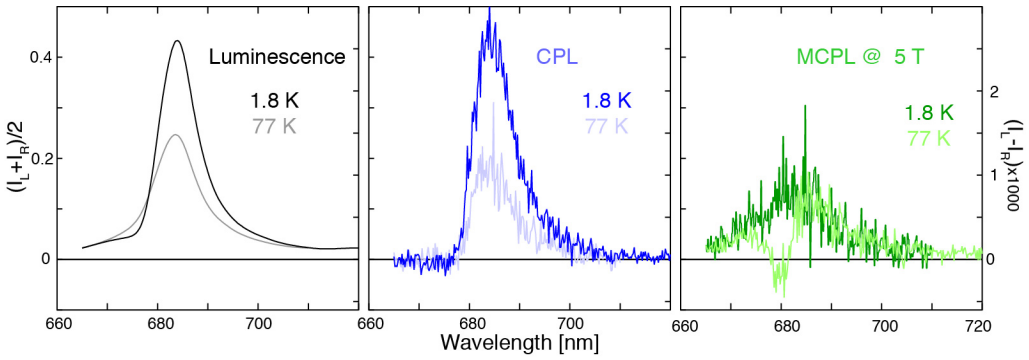

Fig. 4

Luminescence (black, grey) l.h. scale with CPL (blue, light blue) and MCPL at 5T (green, light green) r.h. scale, of RC-6 at 1.8 K and 77 K respectively.

When MCPL spectra are taken at 77 K, the puzzling negative MCPL feature seen at 1.8 K is not evident (see Fig. 4). The main luminescence peak becomes weaker at 77 K but apart from some broadening, changes little. There is even less change in the free *Chl-a* luminescence component and its MCPL is also unchanged.

Whereas chlorins display a *positive* MCD/MCPL of their (lowest energy) Q_y state, tetrapyrroles in general, as characterised by the four-orbital model of Gouterman [23], can have a very wide range of magneto-optical properties, including instances [24] where the lowest excited state shows a strong negative MCD (and thus MCPL). The observation of a strongly negative, relatively sharp MCPL feature in RC-6 with little CPL and no analogous feature in absorption, suggests the possibility that the unique excited state photoactivity of RC-6 may create a short-lived excited state transient species responsible for the feature observed. We propose that by 77 K the lifetime of the transient species has become shorter and thus contributes less to the luminescence.

Exciton Modelling of RCs

The electronic structure of RCs can be modelled using an exciton coupling model. The pairwise interaction $\hat{V}_{ab}$ couples the transition dipole moments $\tilde{\mu}_{a,b}$, each centred at a *Chl-a* or *Pheo-a*, separated by r_{ab}.

$$\hat{V}_{ab} = (\tilde{\mu}_a \cdot \tilde{\mu}_b) - 3(\tilde{\mu}_a \cdot r_{ab})(\tilde{\mu}_b \cdot r_{ab})\, r_{ab}^{-3} \qquad (3)$$

For all 8 pigments in an RC, an 8 x 8 Hamiltonian matrix is created. The diagonal elements are the (uncoupled) site energies of each pigment. The off-diagonal components $\hat{V}_{ab}$ are the coupling terms between each pair of pigments. The magnitude and direction of the Q_y transition dipoles can be experimentally determined for isolated, monomeric *Chl-a* and *Pheo-a*. Here, we use the same transition dipoles and recently-determined coupling matrix $\hat{V}_{ab}$ as in reference [25] (also shown in Table S3). Structural data is obtained from the x-ray crystal structure reported in reference [26] to provide the relative distances and orientations of the transition dipoles.

Each site energy is attributed a Gaussian-shaped spectral width to account for inhomogeneous broadening. However, variations in the site energy of one pigment are *not correlated* with those of other pigments. This leads to the situation where the *relative* site energies of pigments can have a range of realisations with markedly distinct electronic characteristics. A similar phenomenon occurs [27] for the series of inorganic complexes $Ir(bpy)_x(phen)_{3-x}$, x=0-3 where two distinct luminescences (dual luminescence) are observed in frozen solution spectra of the x=1 and x=2 cases. In RCs, inhomogeneous broadening is comparable to differences in site energy and the relative order of the two lowest-energy exciton eigenstates can be 'inverted' compared to normal for a subset of realisations [28].

To fully account for non-correlation, a large number of realisations (>10^6) need to be included to effectively model spectra. This is done by varying site energies over their inhomogeneous (and non-correlated) distributions and then adding each contribution to a total spectrum, each realisation being weighted by its probability. We approximate the influence of phonon wings at 0 K by attributing a Gaussian width of 30 cm^{-1} to each exciton eigenstate. We do not account for thermal motions by coupling excitations to the thermal bath. This needs to be done to account for the temperature dependence of spectra in more detailed calculations. We further reduce the time needed for the computational modelling by noting that coupling terms between the ChlZ pigments and other pigments are very small. Neglecting coupling to ChlZ pigments reduces the size of the Hamiltonian matrix to be repetitively diagonalised to 6 x 6.

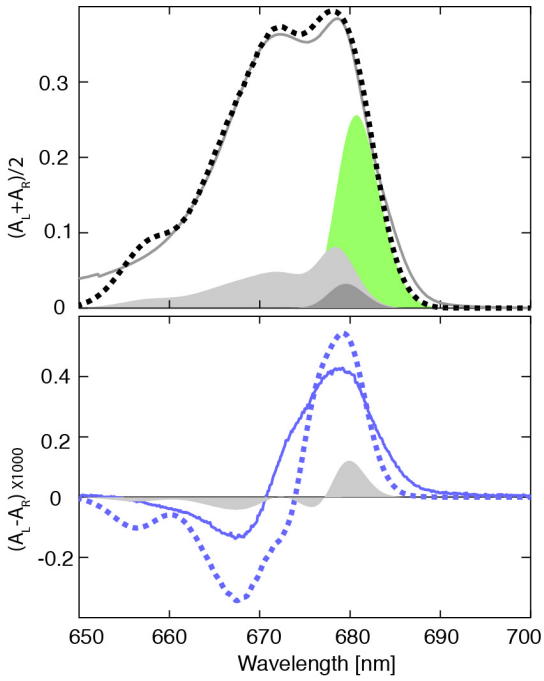

Fig. 5

The upper panel shows the 1.8 K absorption spectrum of RC-6 (grey trace) along with the absorption line-shape (dotted black trace) calculated using the parameters described in the text and the SI. The lower panel shows the simultaneously measured experimental CD spectrum (blue trace) and the computed CD spectrum (dotted blue trace). In the upper panel, the green envelope is the distribution of lowest energy exciton realisation, whilst the smaller dark grey envelope is the distribution of the lowest energy exciton of the inverted population, i.e. where the lowest exciton is dominantly Pheo$_{D2}$. The light grey envelope is the calculated absorption profile of the inverted population. The light grey envelope in the lower panel is the corresponding calculated CD of the inverted population.

Fig. 5 shows a comparison of calculated and experimental absorption and CD spectra of RC-6, using the parameters given in Tables S2 and S3. Both experimental and theoretical spectra are similar to those previously presented [6b, 7b, 29]. However, we have introduced a number of new features to the analysis.

Firstly, the site energy and width of ChlZ$_{D1}$ is not parameterised but experimentally determined by means of the subtraction of spectra of RC-6 and RC-5 scaled per reaction centre. The coupling between ChlZ pigments and other RC pigments is small (Table S3) and thus the excitonic effects of removing it on other RC pigments is minimal. It has been shown that the MCD magnitude of ChlZ$_{D1}$ is very similar to that of *Chl-a* in ether and that the RC- 6 minus RC-5 spectral profile provides a good model for the Q_y spectrum of an isolated *Chl-a* with known axial coordination [1c]. ChlZ$_{D2}$ was taken to have the same width as ChlZ$_{D1}$ and its spectral position adjusted to reproduce the experimental absorption profile.

Secondly, the amplitude of the calculated CD spectrum in Fig 5 has been determined using the appropriate constants that connect absorption and CD spectra to calculated rotational strength. The CD is not arbitrarily scaled, as has been done in previous comparisons of experimental and calculated spectra. This assists in identifying regions of the CD spectrum that may be responsible for the overall non-conservative characteristics seen. Particularly useful is a quantitative comparison of the CD spectra of RC-6 and RC-5, when scaled per PS II reaction centre (Fig 6 and Fig S2). This establishes that $ChlZ_{D1}$ contributes minimally to the overall CD. This result is consistent with the fact that $ChlZ_{D1}$ interacts only weakly with other pigments in the RC.

Thirdly, we have identified a single set of site energies and widths that is able to account for absorption and CD spectra of *both* RC-6 and RC-5 reasonably well. Absorption and CD for each Q_y exciton realisation are shown in Fig. 6. Also shown are the absorption and CD of exciton realisations where $Pheo_{D2}$ dominates the lowest energy exciton, i.e. for the inverted population. As the same site energies and widths are used for all pigments except for (uncoupled) ChlZ contributions, calculated absorption and CD spectra of the interacting pigments are the same for RC-5 and RC-6. The lowest-energy, inverted-population exciton has an intensity of 14% of the lowest exciton for all realisations. This result is in agreement with previous modelling [28] of the absorption spectrum of RC-5.

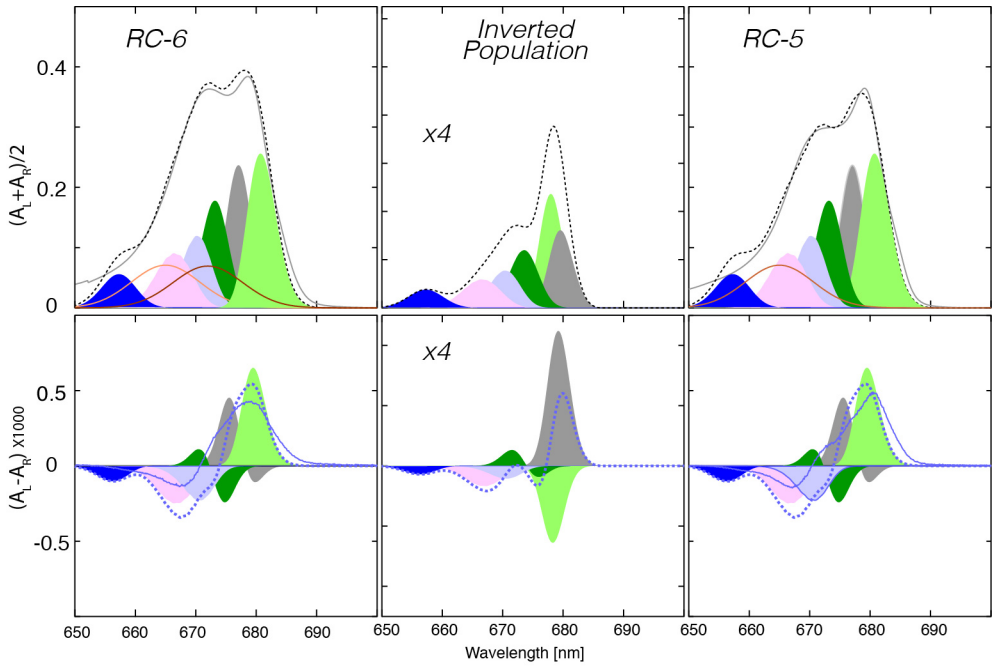

Fig. 6

The l.h. panels and r.h. panels show absorption (upper) and CD (lower) spectra of RC-6 and RC-5 respectively. Experimental absorption and CD spectra (solid grey lines for absorption and solid blue lines for CD) were measured simultaneously. Calculated spectra (dotted lines) use the parameters

shown in Tables S2 and S3. The brown lines are the (uncoupled) ChlZ absorption components. The filled lineshapes are the six exciton components. The centre panel shows calculated absorption and CD spectra of the 6 coupled pigments common to RC-6 and RC-5 for the inverted population, i.e. where the lowest exciton is dominated by $Pheo_{D2}$. Calculated absorption and CD of the inverted population have been scaled by a factor of 4.

The modelling presented in Figs. 5 and 6 highlights the effects of non-correlated heterogeneity in the spectroscopy of RC-6 and RC-5. Close to 15% of all realisations give rise to a predominantly $Pheo_{D2}$ exciton at lowest energy rather than a Chl_{D1}-based exciton. Absorption and CD spectra of the inverted population are distinctly different to that of the entire population. It seems noteworthy that the MCPL anomaly and the MCD deficit both occur in this inverted population spectral region.

Calculated CD of the second and third excitons (nominally identified as involving $Pheo_{D2}$ and $Pheo_{D1}$) do not exhibit the same profile in absorption and CD (Fig. 6). The CD is seen to change sign across an exciton realisation in some cases. In PS II core complexes, site energy heterogeneity is far smaller and thus the effects of non-correlation become more subtle [30].

RC-6 and RC-5 show a very similar non-conservative CD component amplitude. The CD difference spectra shown in Fig. S2 reveal that the change in CD in passing from RC-6 to RC-5 is close to conservative. This may reflect relatively small shifts and linewidth changes in the $Pheo_{D2}/Pheo_{D1}$ region between 675 nm and 681 nm for the two systems. The calculated exciton CD in this region is quite sensitive to small changes. There is virtually no change in the CD in the 650 nm to 670 nm region although the absorption change, owing to the removal of $ChlZ_{D1}$, is significant. Thus, both the excitonic and non-conservative components of the CD in RCs, arise principally from the six central pigments.

The similar amplitude of the calculated and experimental CD in the 680 nm region in RC-5 and RC-6 leads us to suggest that $Chl_{D1}/Pheo_{D1}$ exciton coupling is responsible for the main positive peak seen. This is in spite of the strongest coupling term in PS II reaction centre being between P_{D1} and P_{D2} (Table S3). P_{D1}/P_{D2} dominate the highest energy exciton (dark blue envelope of Fig 6). Reducing the CD contributions of the P_{D1}/P_{D2} excitons (Fig. S3 provides a full set of pigment distributions for each exciton) we can. at least phenomenologically, account for much of the non-conservative nature of the CD seen. It is not clear how this procedure could be theoretically justified but may be related to the fact that only the P_{D1}-P_{D2} pair of pigments experience direct electronic overlap. This direct overlap also gives rise to the optical charge transfer band [31] in PS II core complexes.

5 Conclusions

A comparison of CD and MCD spectra with measurements of CPL and MCPL spectra show that the CPL is compatible with the observed CD. An anomalous feature appears in the MCPL spectrum near 681 nm. This feature is not present in 77 K spectra, which suggests that the anomaly may be due to the formation of a metastable emitting species having very different electronic properties to that of a chlorin.

Exciton modelling of absorption and CD spectra of RC-6 and RC-5 has been improved. A set of site energies, for which the $ChlZ_{D1}$ value was determined from experiment was introduced and applied to both RC-6 and RC-5. A more recent set of structural parameters and a more refined set of coupling energies were also utilised in the modelling. The presence of a substantial (14%) inverted population in the exciton realisations, for which the lowest exciton is predominantly $Pheo_{D1}$ and not Chl_{D1} is consistent with an earlier analysis [28].

A comparison of CD spectra of RC-6 and RC-5 establishes that $ChlZ_{D1}$ has little contribution to the Q_y CD of RC-6 or RC-5. This can also be reasonably assumed to be the case for ChZ_{D2}. The non-excitonic component of the overall CD in the Q_y region can be qualitatively accounted for by neglecting the CD associated with the P_{D1}-P_{D2} special pair exciton realisations.

This work provides clues as to the origin of the non-conservative Q_y CD in RCs. Additionally, MCPL data points to the creation of a metastable species in the excited state of RC-6, which puts interpretation of ps and fs transient experiments on RCs in question.

Supplementary Material

Document provided.

Conflicts of Interest

None

Acknowledgements

The technical support of Keith Jackman is gratefully acknowledged. Julien Langley kindly provided the graphics for Figure 1. Martyna Judd was responsible for determining the correct conversion from rotational strength to CD amplitude and assisted in numerous discussions. We recognise the support of the Australian Research Council through grants DP110104565 and DP150103137 (E.K.).

References

[1] aE. Romero, R. Augulis, V. I. Novoderezhkin, M. Ferretti, J. Thieme, D. Zigmantas, et al. Quantum coherence in photosynthesis for efficient solar-energy conversion. Nat Phys. **2014**, *10*, 677; bF. D. Fuller, J. Pan, A. Gelzinis, V. Butkus, S. S. Senlik, D. E. Wilcox, et al. Vibronic coherence in oxygenic photosynthesis. Nat Chem. **2014**, *6*, 706; cJ. R. Reimers, Z. L. Cai, R. Kobayashi, M. Ratsep, A. Freiberg, E. Krausz. Assignment of the Q-Bands of the Chlorophylls: Coherence Loss via Qx - Qy Mixing. Sci Rep. **2013**, *3*, 2761.

[2] aD. J. Nurnberg, J. Morton, S. Santabarbara, A. Telfer, P. Joliot, L. A. Antonaru, et al. Photochemistry beyond the red limit in chlorophyll f-containing photosystems. Science. **2018**, *360*, 1210; bT. Renger, E. Schlodder. The primary electron donor of photosystem II of the cyanobacterium Acaryochloris marina is a chlorophyll d and the water oxidation is driven by a chlorophyll a/chlorophyll d heterodimer. Journal of Physical Chemistry B. **2008**, *112*, 7351; cM. R. Razeghifard, M. Chen, J. L. Hughes, J. Freeman, E. Krausz, T. Wydrzynski. Spectroscopic Studies of Photosystem II in Chlorophyll *d*-containing *Acaryochloris marina*. Biochemistry. **2005**, *44*, 11178.

[3] T. Wydrzynski, K. Satoh. *Photosystem II - The Light-Driven Water:Plastoquinone Oxidoreductase in: Govindjee (series ed), Advances in Photosynthesis and Respiration Vol. 22 pp 786. Springer, Dordrecht, The Netherlands.* **2005**.

[4] O. Nanba, K. Satoh. Isolation of a Photosystem II Reaction Center Consisting of D-1 and D-2 Polypeptides and Cytochrome *b*-559. Proceedings of the National Academy of Sciences. **1987**, *84*, 109.

[5] V. L. Tetenkin, B. A. Gulyaev, A. B. Rubin, M. Seibert. Spectral Properties of Isolated Photosystem-Ii Reaction Center Complex at 77k. Current Research in Photosynthesis, Vols 1-4. **1990**, A427.

[6] aG. Raszewski, W. Saenger, T. Renger. Theory of Optical Spectra of Photosystem II Reaction Centers: Location of the Triplet State and the Identity of the Primary Electron Donor. Biophysical Journal. **2005**, *88*, 986; bG. Raszewski, B. A. Diner, E. Schlodder, T. Renger. Spectroscopic properties of reaction center pigments in photosystem II core complexes: Revision of the multimer model. Biophysical Journal. **2008**, *95*, 105.

[7] aV. I. Novoderezhkin, E. G. Andrizhiyevskaya, J. P. Dekker, R. van Grondelle. Pathways and Timescales of Primary Charge Separation in the Photosystem II Reaction Center as Revealed by a Simultaneous Fit of Time-Resolved Fluorescence and Transient Absorption. Biophys J. **2005**, *89*, 1464; bA. Gelzinis, D. Abramavicius, J. P. Ogilvie, L. Valkunas. Spectroscopic properties of photosystem II reaction center revisited. Journal of Chemical Physics. **2017**, *147*.

[8] K. Acharya, V. Zazubovich, M. Reppert, R. Jankowiak. Primary Electron Donor(s) in Isolated Reaction Center of Photosystem II from Chlamydomonas reinhardtii. J Phys Chem B. **2012**.

[9] H. Ago, H. Adachi, Y. Umena, T. Tashiro, K. Kawakami, N. Kamiya, et al. Novel Features of Eukaryotic Photosystem II Revealed by Its Crystal Structure Analysis from a Red Alga. Journal of Biological Chemistry. **2016**, *291*, 5676.

[10] aJ. Hall, T. Renger, R. Picorel, E. Krausz. Circularly polarized luminescence spectroscopy reveals low-energy excited states and dynamic localization of vibronic transitions in CP43. Biochim Biophys Acta. **2016**, *1857*, 115; bJ. Hall, T. Renger, F. Muh, R. Picorel, E. Krausz. The lowest-energy chlorophyll of photosystem II is adjacent to the peripheral antenna: Emitting states of CP47 assigned via circularly polarized luminescence. Biochim Biophys Acta. **2016**, *1857*, 1580.

[11] J. R. Reimers, M. Biczysko, D. Bruce, D. F. Coker, T. J. Frankcombe, H. Hashimoto, et al. Challenges facing an understanding of the nature of low-energy excited states in photosynthesis. Biochim Biophys Acta. **2016**.

[12] S. B. Piepho, P. N. Schatz. *Group Theory in Spectroscopy with Applications to Magnetic Circular Dichroism* **1983** (Wiley-Interscience: New York, Chichester, Brisbane, Toronto, Singapore).

[13] aT. Nozawa, M. Kobayashi, Z. Y. Wang, S. Itoh, M. Iwaki, M. Mimuro, et al. Magnetic Circular Dichroism Investigation on Chromophores in Reaction Centres of Photosystem I and II of Green Plant Photosynthesis. Spectrochimica Acta. **1995**, *51A*, 125; bM. Mimuro, M. Kobayashi, K. Shimada, K. Uezono, T. Nozawa. Magnetic Circular Dichroism Properties of Reaction Centre Complexes Isolated from the Zinc-Bacteriochlorophyll *a*-containing Bacterium *Acidiphilium rubrum*. Biochemistry. **2000**, *39*, 4020; cM. Umetsu, R. Seki, Z.-Y. Wang, I. Kumagai, T. Nozawa. Circular and Magnetic Circular Dichroism Studies of Bacteriochlorophyll *c* Aggregates: T-Shaped and Antiparallel Dimers. Journal of Physical Chemistry B. **2002**, *106*, 3987; dP. J. Smith, E. Krausz, V. M. Masters, T. Wydrzynski, S. Peterson, S. Styring, et al. in *PS2001 PROCEEDINGS: 12th International Congress on Photosynthesis* **2001,** (CSIRO Publishing: Brisbane); eS. P. Årsköld, P. J. Smith, J.-R. Shen, R. J. Pace, E. Krausz. Key cofactors of Photosystem II cores from four organisms identified by 1.7-K absorption, CD and MCD. Photosynth Res. **2005**, *84*, 309; fJ. L. Hughes, R. Razeghifard, M. Logue, A. Oakley, T. Wydrzynski, E. Krausz. Magneto-Optic Spectroscopy of a Protein Tetramer Binding Two Exciton-Coupled Chlorophylls. Journal of the American Chemical Society. **2006**, *128*, 3649.

[14] aD. Zevenhuijzen, P. J. Zandstra. Absorption and Magnetic Circular Dichroism of Chlorophyll *a* and *b* Dimers. Biophysical Chemistry. **1984**, *19*, 121; bJ. L. Hughes, R. J. Pace, E. Krausz. The Exciton Contribution to the Faraday B term MCD of Molecular Dimers. Chemical Physics Letters. **2004**, *385*, 116.

[15] E. Krausz, J. L. Hughes, P. Smith, R. Pace, S. Peterson Årsköld. Oxygen-Evolving Photosysten II Core Complexes: A New Paradigm Based on the Spectral Identification of the Charge-Separating State, the Primary Acceptor and Assignment of Low-Temperature Fluorescence. Photochemical and Photobiological Sciences. **2005**, *4*, 744.

[16] aE. Krausz. Selective and Differential Optical Spectroscopies in Photosynthesis. Photosynthesis Research. **2013**; bJ. Morton, F. Akita, Y. Nakajima, J.-R. Shen, E. Krausz. Optical identification of the long-wavelength (700–1700nm) electronic excitations of the native reaction centre, Mn4CaO5 cluster and cytochromes of photosystem II in plants and cyanobacteria. Biochimica et Biophysica Acta (BBA) - Bioenergetics. **2015**, *1847*, 153; cJ. Morton, M. Chrysina, V. S. J. Craig, F. Akita, Y. Nakajima, W. Lubitz, et al. Structured near-infrared Magnetic Circular Dichroism spectra of the Mn4CaO5 cluster of PSII in T. vulcanus are dominated by Mn(IV) d-d 'spin-flip' transitions. Bba-Bioenergetics. **2018**, *1859*, 88.

[17] J. L. Hughes, E. Krausz. in *Application of Physical Methods to Inorganic and Bioinorganic Chemistry* Eds. Scott RA, Lukehart CM) **2007**, (John Wiley & Sons, Ltd.).

[18] M. Seibert, R. Picorel. in *Photosynthesis Research Protocols* (Ed. Carpentier R) **2011**, (Humana Press, Pringer: New York, Heidelberg, London.).

[19] E. Krausz, N. Cox, S. P. Arskold. Spectral characteristics of PS II reaction centres: as isolated preparations and when integral to PS II core complexes. Photosynthesis Research. **2008**, *98*, 207.

[20] M. Germano, A. Y. Shkuropatov, H. Permentier, R. d. Wijn, A. J. Hoff, V. A. Shuvalov, et al. Pigment Organization and Their Interactions in Reaction Centers of Photosystem II: Optical Spectroscopy at 6K of Reaction Centers with Modified Pheophytin Composition. Biochemistry. **2001**, *40*, 11472.

[21] C. Houssier, K. Sauer. Circular Dichriosm and Magnetic Circular Dichroism of the Chlorophyll and Protochlorophyll Pigments. Journal of the American Chemical Society. **1970**, *92*, 779.

[22] aP. J. Smith, S. Peterson, V. M. Masters, T. Wydrzynski, S. Styring, E. Krausz, et al. Magneto-Optical Measurements of the Pigments in Fully Active Photosystem II Core Complexes from Plants. Biochemistry. **2002**, *41*, 1981; bS. Peterson Årsköld, V. M. Masters, B. J. Prince, P. J. Smith, R. J. Pace, E. Krausz. Optical Spectra of Synechocystis and Spinach Photosystem II Preparations at 1.7 K: Identification of the D1-Pheophytin Energies and Stark Shifts. Journal of the American Chemical Society. **2003**, *125*, 13063.

[23] aM. Gouterman. A Theory for the Spectral Variations among the Metal Porphyrins. Spectrochimica Acta. **1957**, *10*, 232; bM. Gouterman. Spectra of Porphyrins. Journal of Molecular Spectroscopy. **1961**, *6*, 138; cM. Gouterman, L. C. Snyder, G. H. Wagniere. Spectra of Porphyrins .2. 4 Orbital Model. Journal of Molecular Spectroscopy. **1963**, *11*, 108.

[24] aM. R. Cheesman, C. Greenwood, A. J. Thomson. Magnetic Circular-Dichroism of Hemoproteins. Adv Inorg Chem Rad. **1991**, *36*, 201; bJ. Mack, M. J. Stillman, N. Kobayashi. Application of MCD spectroscopy to porphyrinoids. Coordination Chemistry Reviews. **2007**, *251*, 429.

[25] F. Muh, M. Plockinger, T. Renger. Electrostatic Asymmetry in the Reaction Center of Photosystem II. J Phys Chem Lett. **2017**, *8*, 850.

[26] Y. Umena, K. Kawakami, J. R. Shen, N. Kamiya. Crystal structure of oxygen-evolving photosystem II at a resolution of 1.9 angstrom. Nature. **2011**, *473*, 55.

[27] E. Krausz, J. Higgins, H. Riesen. The apparent "dual emitter" characteristics of iridium bipyridine phenanthroline complexes, [Ir(bpy)x(phen)3-x]3+ for x = 1,2. Inorganic Chemistry. **1993**, *32*, 4053.

[28] N. Cox, J. Hughes, A. W. Rutherford, E. Krausz. On the assignment of PSHB in D1/D2/cytb(559) reaction centers. Physcs Proc. **2010**, *3*, 1601.

[29] aT. Renger. Theory of Optical Spectra involving Charge Transfer States: Dynamic Localization Predicts a Temperature Dependent Optical Band Shift. Physical Review Letters. **2004**, *93*, 188101; bJ. Adolphs, F. Muh, M. E. A. Madjet, M. S. A. Busch, T. Renger. Structure-Based Calculations of Optical Spectra of Photosystem I Suggest an Asymmetric Light-Harvesting Process. Journal of the American Chemical Society. **2010**, *132*, 3331; cV. I. Novoderezhkin, J. P. Dekker, R. van Grondelle. Mixing of Exciton and Charge-Transfer States in Photosystem II Reaction Centers: Modeling of Stark Spectra with Modified Redfield Theory. Biophys J. **2007**, *93*, 1293.

[30] N. Cox, J. L. Hughes, R. Steffen, P. J. Smith, A. W. Rutherford, R. J. Pace, et al. Identification of the Q(Y) Excitation of the Primary Electron Acceptor of Photosystem II: CD Determination of Its Coupling Environment. Journal of Physical Chemistry B. **2009**, *113*, 12364.

[31] J. L. Hughes, P. Smith, R. Pace, E. Krausz. Charge Separation in Photosystem II Core Complexes Induced by 690-730 nm Excitation at 1.7 K. Biochimica et Biophysica Acta. **2006**, *1757*, 841.

Supplementary Information

New Perspectives on Photosystem II Reaction Centres

Jeremy Hall[A], *Rafael Picorel*[B], *Nicholas Cox*[A], *Robin Purchase*[A] *and Elmars Krausz*[A]

[A] Research School of Chemistry, Australian National University, Canberra, Australia

[B] Estacion Experimental de Aula Dei (CSIC), Avda. Montañana 1005, 50059-Zaragoza, Spain

Email: elmars.krausz@anu.edu.au Fax:+61-2-6125-0

SI Global Fitting of Luminescence, CPL and MCPL spectra

Attempts were made to simultaneously fit the luminescence, CPL and MCPL spectra with three Gaussian profiles. These correspond to the main luminescence peak at 685 nm, a broader free *Chl-a* component centred near 671 nm and an anomalous, relatively narrow peak at 681 nm. The latter is needed mainly to account for the negative MCPL feature. The main luminescence peak lineshape is not well accounted for as it clearly deviates from Gaussian, but a reasonable account of the overall spectral profiles can be provided, which enables an estimate of the relative areas of the components in the luminescence, CPL and MCPL spectra. These are provided in Fig S1 and Table S1.

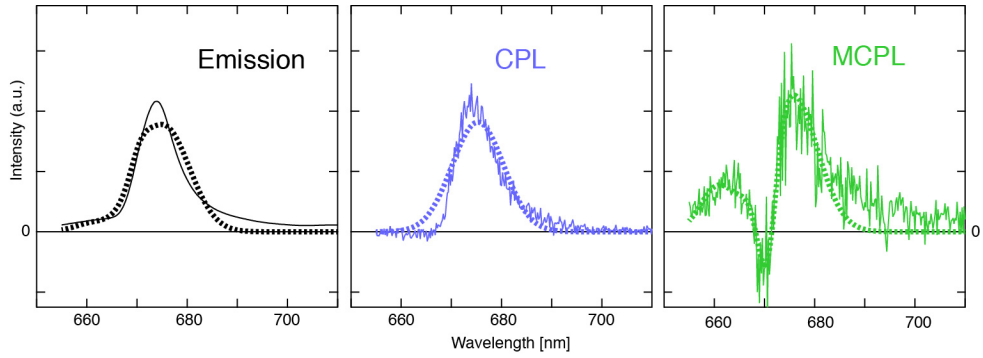

Fig. S1
Luminescence (black) CPL (light blue) and MCPL at 1 T (light green) of RC-6 at 1.8 K, scaled by factors of 1, 1600 and 20000 together with the global fit (thicker dashed curves) *to three Gaussians (See Table S1)*

Table S1

Global fit parameters of Luminescence, CPL and MCPL spectra in Fig. S4 to the Sum of Three Gaussians

Position nm/ (FWHM cm^{-1})	Luminescence	CPL	MCPL
671/(150)	Amplitude=3.7 x 10^{-3} Area=1.8 x 10^{-2} Relative area=0.066	Amplitude=0 ρ_E=0	Amplitude=5.4 x 10^{-6} 1T ρ_E=0.28 x 10^{-3}
681/(100)	Amplitude = 9.8 x 10^{-3} Area=3.1 x 10^{-2} Relative area = 0.115	Amplitude=0 ρ_E=0	Amplitude=-1.2 x 10^{-5} 1T ρ_E=-0.26 x 10^{-3}
685/(190)	Amplitude=3.6 x 10^{-2} Area=0.22 Relative area=0.819	Amplitude=2.5 x 10^{-5} ρ_E=0.69 x 10^{-3}	Amplitude=1.7 x 10^{-5} 1T ρ_E=0.1 x 10^{-3}

SI Exciton Modelling of Absorption and CD spectra of RC-6 and RC-5

Table S2

*RC-5 & RC-6 Site Parameters**

	Site Energy (nm)	FWHM (cm^{-1})
Chl_{D1}	680	140
$Pheo_{D2}$	676	140
$Pheo_{D1}$	669	220
P_{D1}	665.5	220
P_{D2}	665.5	220
Chl_{D2}	669	220
$ChlZ_{D1}$	672	300
$ChlZ_{D2}$	665	300

**The site parameters used for RC5 and RC6 are identical, except that RC5 lacks $ChlZ_{D1}$ at 672 nm. The spectral position and width of $ChlZ_{D1}$ was taken from the subtraction [1] of scaled spectra of RC-6 and RC-5.*

Table S3

PSII RC Coupling matrix[2]

Coupling (cm^{-1})	Chl_{D1}	$Pheo_{D2}$	$Pheo_{D1}$	P_{D1}	P_{D2}	Chl_{D2}	$ChlZ_{D1}$	$ChlZ_{D2}$
Chl_{D1}	0	-2.18	43.51	-27.32	-46.77	3.54	1.67	-0.09
$Pheo_{D2}$	-2.18	0	1.55	12.61	-2.99	41.65	-0.19	-2.57
$Pheo_{D1}$	43.51	1.55	0	-3.96	15.06	-2.37	-2.52	-0.18
P_{D1}	-27.32	12.61	-3.96	0	158	-41.83	0.45	0.58
P_{D2}	-46.77	-2.99	15.06	158	0	-22.04	0.6	0.61
Chl_{D2}	3.54	41.65	-2.37	-41.83	-22.04	0	-0.05	1.8
$ChlZ_{D1}$	1.67	-0.19	-2.52	0.45	0.6	-0.05	0	0.15
$ChlZ_{D2}$	-0.09	-2.57	-0.18	0.58	0.61	1.8	0.15	0

Transition Dipole strengths were taken[2] as 5.47 D for chl-a and 4.25 D for pheo-a.

SI Quantitative Absorption and CD comparison of RC-6 with RC-5

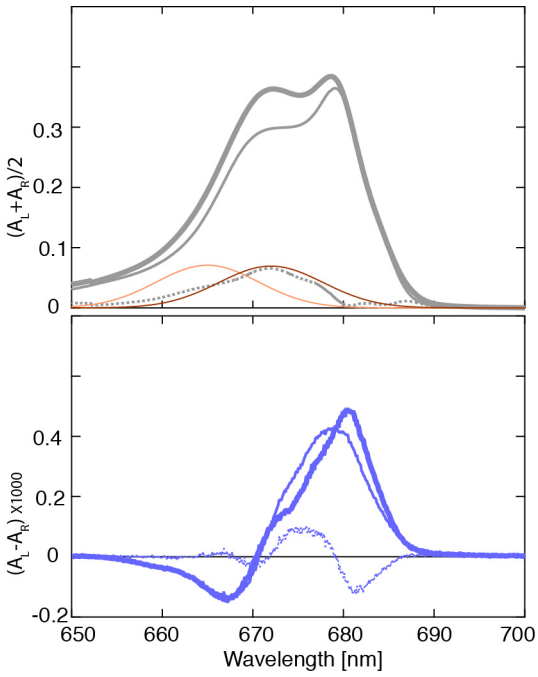

Fig. S2

The top and bottom panels compare the absorption (grey) and CD (blue) spectra of RC-6 (thick) and RC-5 (thin) respectively. Spectra are scaled to two pheo-a molecules per RC, i.e. the same number of reaction centres. Also shown are difference spectra (dotted lines), as well as the modelled absorptions of $ChlZ_{D1}$ (dark brown) and $ChlZ_{D2}$ (light brown).

SI Pigment Distribution of RC excitons

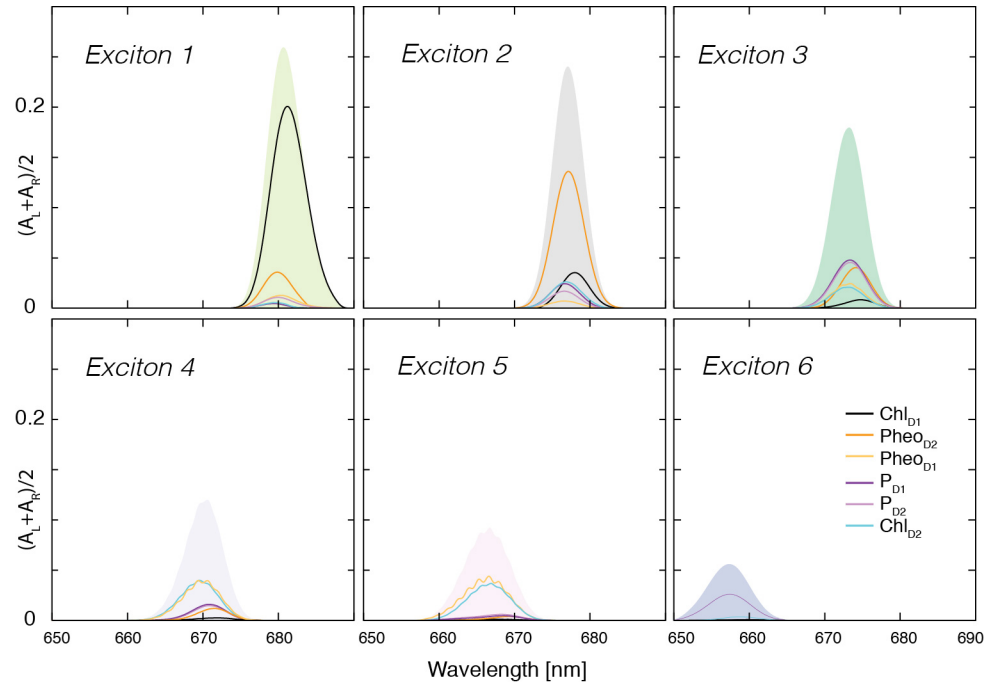

Fig. S3

The pigment distribution of the six excitons of RC-6 and RC-5 in Fig. 6 of the main text are shown in the six panels of the figure. Each filled and coloured profile is one of the excitons. The coloured lines within each profile shows the contribution of each coupled pigment. The colour coding used for pigments in Exciton 6 applies to all excitons.

The pigment distributions shown in Fig. S3 identify which pigments contribute significantly to each exciton. For example, Chl_{D1} dominates Exciton 1 and Exciton 6 is an equal mixture of P_{D1} and P_{D2}. Note that the distribution of each pigment varies and may not have the same lineshape as the exciton itself. This is due to the non-correlated heterogeneity of pigment energies. A less detailed pigment distribution is provided in Fig. 4 of the pioneering 2008 paper[3] by the Renger group.

Supplementary References:

[1] aE. Krausz, N. Cox, S. P. Arskold. Spectral characteristics of PS II reaction centres: as isolated preparations and when integral to PS II core complexes. Photosynthesis Research. **2008**, *98*, 207; bJ. R. Reimers, Z. L. Cai, R. Kobayashi, M. Ratsep, A. Freiberg, E. Krausz. Assignment of the Q-Bands of the Chlorophylls: Coherence Loss via Qx - Qy Mixing. Sci Rep. **2013**, *3*, 2761.

[2] F. Muh, M. Plockinger, T. Renger. Electrostatic Asymmetry in the Reaction Center of Photosystem II. J Phys Chem Lett. **2017**, *8*, 850.

[3] G. Raszewski, B. A. Diner, E. Schlodder, T. Renger. Spectroscopic properties of reaction center pigments in photosystem II core complexes: Revision of the multimer model. Biophysical Journal. **2008**, *95*, 105.